Alexandria Engineering Journal 91 (2024) 249–260

Contents lists available at ScienceDirect

Alexandria Engineering Journal

journal homepage: www.elsevier.com/locate/aej

Original Article

# An energy-aware routing scheme based on a virtual relay tunnel in flying ad hoc networks

Mehdi Hosseinzadeh [a,b], Saqib Ali [c], Adil Hussein Mohammed [d], Jan Lansky [e], Stanislava Mildeova [e], Mohammad Sadegh Yousefpoor [f], Efat Yousefpoor [f], Omed Hassan Ahmed [g], Amir Masoud Rahmani [h,*], Asif Mehmood [i]

[a] Institute of Research and Development, Duy Tan University, Da Nang, Viet Nam
[b] School of Medicine and Pharmacy, Duy Tan University, Da Nang, Viet Nam
[c] Department of Information Systems, College of Economics and Political Science, Sultan Qaboos University, Al Khoudh, Muscat, Oman
[d] Department of Communication and Computer Engineering, Faculty of Engineering, Cihan University-Erbil, Kurdistan Region, Iraq
[e] Department of Computer Science and Mathematics, Faculty of Economic Studies, University of Finance and Administration, Prague, Czech Republic
[f] Department of Computer Engineering, Dezful Branch, Islamic Azad University, Dezful, Iran
[g] Department of Information Technology, University of Human Development, Sulaymaniyah, Iraq
[h] Future Technology Research Center, National Yunlin University of Science and Technology, Yunlin, Taiwan
[i] Department of Biomedical Engineering, Gachon University, Seongnam-si, Gyeonggi-do 13120, Republic of Korea

A R T I C L E I N F O

*Keywords:*
Flying ad hoc networks (FANETs)
Routing
Artificial Intelligence (AI)
Drone
Wireless network

A B S T R A C T

Flying ad hoc networks (FANETs) tackle diverse challenges, for example, dynamic topological structure, high mobility of nodes, low density, and energy restrictions. These challenges make problems in designing reliable and stable routing in FANETs. Hence, the design of a routing algorithm is essential for transferring data between drones. In this paper, an energy-aware routing scheme based on a virtual relay tunnel (EARVRT) is proposed in flying ad hoc networks. EARVRT includes a virtual relay tunnel (VRT) that manages relay nodes in the route discovery process and lowers network overhead. Moreover, three metrics, namely route energy, hop counts, and a new metric called path correlation are regarded in the path selection operation. Note that correlation is defined with regard to two scales, including the cosine similarity of two nodes and their distance. EARVRT is evaluated according to delay, network longevity, consumed energy, and packet delivery rate. Then, our scheme is compared with three methods, namely LoCaL, O-LAR, and PSO-GLFR. These results show the superiority and success of EARVRT in comparison with other algorithms.

## 1. Introduction

Nowadays, most military and civilian applications can be improved using flying ad hoc networks (FANETs). These networks include a number of unmanned aerial vehicles (UAVs), which work together and forward the collected information to the ground control system (GCS) via multi-hop communications [1,2]. FANETs are a member of mobile ad hoc networks (MANETs) and vehicular ad hoc networks (VANETs). FANET is widely used in military and civilian areas. Some examples of FANET applications include public protection, rescue missions in disasters, reconnaissance missions, border control, fire management, agriculture, remote sensing, and traffic monitoring [3,4]. In a multi-UAV network, unlike a single-UAV network, network communications are fault tolerant, meaning that these communications are maintained even though some UAVs fail. In FANET, communications are categorized into two classes, namely UAV-to-UAV (U2U) and UAV-to-GCS (U2G) [5,6].

These networks utilize specific features, for example, very dynamic topology, high mobility, low density, energy restriction, and limited storage capacity [7,8]. For this reason, reliable data transfer and the maintenance of communication links are very important in FANETs. To maintain the stability of routes in the packet transfer process, despite frequent changes in network topology, designing a proper routing

* Corresponding author.
*E-mail addresses:* mehdihosseinzadeh@duytan.edu.vn (M. Hosseinzadeh), saqib@squ.edu.com (S. Ali), adil.mohammed@cihanuniversity.edu.iq (A.H. Mohammed), lansky@mail.vsfs.cz (J. Lansky), 31289@mail.vsfs.cz (S. Mildeova), ms.yousefpoor@iaud.ac.ir (M.S. Yousefpoor), eyousefpoor@iaud.ac.ir (E. Yousefpoor), omed.hassan@uhd.edu.iq (O. Hassan Ahmed), rahmania@yuntech.edu.tw (A.M. Rahmani), asif@gachon.ac.kr (A. Mehmood).

https://doi.org/10.1016/j.aej.2024.02.006
Received 24 April 2023; Received in revised form 25 August 2023; Accepted 5 February 2024
Available online 14 February 2024

protocol is necessary because communication links in the network are extremely unstable due to the features mentioned above, and the dynamic movement of drones in the three-dimensional network space can lead to their failure [9,10].

The ad hoc on-demand distance vector routing protocol (AODV) [20] is a traditional routing protocol designed based on an on-demand technique, which performs the route discovery process only if UAVs disseminate route requests. However, AODV has serious challenges in FANET because this protocol is not designed based on the mentioned specific features of FANETs, especially high mobility of drones and unstable links. The route discovery process introduced in AODV has high delay and routing overhead that make serious problems, especially broadcast storms, and threaten network performance. To increase the adaptability and efficiency of this protocol in FANETs, the geographic location information of drones obtained from positioning systems such as GPS can be used [21,22]. Additionally, the energy level of drones significantly affects the route construction and next-hop selection processes. Therefore, low-energy drones should not participate in the routing process because their energy capacity is not enough to carry out routing operations such as route discovery, route update, and route maintenance. Due to the relatively high distance between drones, the energy capacity of UAVs is typically used to support the long transmission range. This can quickly discharge the limited energy capacity. Hence, UAVs have to save energy to support a long flight time, routing operations, and other tasks. Therefore, FANETs need an energy-aware routing approach that considers the dynamic nature of drones and improves network performance [23,24].

In this paper, an energy-aware routing scheme based on a virtual relay tunnel (EARVRT) is suggested in FANETs. EARVRT modifies AODV and defines a new concept called Virtual Relay Tunnel (VRT) to solve two main problems of AODV, namely high routing overhead and broadcast storm. The main purpose of the proposed protocol is to reduce the number of unnecessary control packets. EARVRT seeks to produce more effective and stable paths through the VRT tunnel. The most important innovations of EARVRT are stated below:

- In EARVRT, the route discovery procedure is based on a virtual tunnel between source and destination. This virtual tunnel restricts the search space in the network and reduces routing overhead because only the drones inside the tunnel space are allowed to broadcast the route request (RREQ) message, other drones remove this message and do not participate in the routing process. This will greatly prevent the broadcast storm in the network. The creation of this tunnel is very fast and does not impose any extra overhead.
- In EARVRT, a new metric called path correlation has been introduced. This parameter is calculated based on the two scales, including the cosine similarity of two nodes and their distance.
- In EARVRT, the template of RREQ message includes various fields, including path energy and route correlation. Finally, the routing path is calculated according to path energy, the number of hops, and path correlation.
- EARVRT is simulated in NS2, and its performance is evaluated in terms of five criteria, namely energy consumption, packet delivery rate, network longevity, overhead, and delay compared with LoCaL, O-LAR, and PSO-GLFR.

The organization of our paper is as follows: Section 2 describes different routing schemes in FANETs. Section 3 states the network assumptions in EARVRT. Section 4 explains EARVRT. Section 5 includes the simulation and evaluation results. Section 6 presents the conclusion.

## 2. Related works

In [11], a load-balanced and optimized predictive and adaptive routing (LB-OPAR) approach is proposed for FANET. LB-OPAR is an SDN-based algorithm, which modifies the OPAR algorithm. SDN-based routing schemes can successfully manage the FANET environment. LB-OPAR distributes a balanced load between nodes to get better network performance in terms of throughput, success rate, and flow finishing time. The authors have analytically examined the routing issue in FANET and suggested a suitable routing solution, which considers hop counts, path longevity, and network load. The authors have also analyzed the time complexity of the proposed solution. LB-OPAR presents a very precise and lightweight technique to estimate link duration. The experiments prove that LB-OPAR has high throughput and suitable flow finishing time.

In [12], an intelligent cluster-based routing approach (ICRA) is designed for FANETs. This approach has three items: clustering, clustering settings, and routing. In the first item, each node computes a utility value to decide on cluster heads. Four utility factors, including current energy, centrality, the similarity of speeds of nodes, and link duration time are considered for obtaining the final utility value. The clustering setting item is responsible for adjusting the weight of factors used in the fitness value. This item utilizes reinforcement learning to enhance network stability and longevity. ICRA has benefited the learning process to achieve the best strategy for calculating the utility value in a particular state. Hence, this item can specify the optimal cluster heads with regard to the current network state. In the routing process, ICRA proposes inter-cluster nodes, which are responsible for exchanging data packets between clusters. This strategy lowers delay and increases packet delivery. The experimental results show that ICRA presents a successful clustering strategy, which leads to network stability, high quality of services (QoS), and energy efficiency.

In [13], a resilient Q-learning-based routing algorithm called TARRAQ is suggested in FANETs to exactly record topology changes and decide on routing paths in a decentralized and independent manner. In TARRAQ, the behavior of flying nodes is analyzed using the queuing theory to extract two parameters, namely the neighbor's change rate (NCR) and neighbor's change time (NCIT). Then, these two parameters are used to specify a resilient evaluation interval based on the latency expected to network events. Additionally, drones utilize an adaptive Q-learning approach to decide on routing paths using a decentralized, independent, and adaptive manner in which the action and state spaces will be refreshed in a short time and with little cost. The simulation results confirm the high accuracy of the model presented in TARRAQ and prove that this approach protocol works better than other schemes with regard to overhead, energy, and packet delivery ratio.

In [14], the authors improved the optimized link state routing (OLSR) and presented a fuzzy logic-based routing approach called OLSR+ in FANET. This protocol is made up of four components: 1) Finding neighbors. This component evaluates the longevity of the link between two flying nodes using an effective solution, which takes into account distance, communication quality, movement direction, and relative speed. 2) Choosing multi-point relays (MPRs). This component designs a fuzzy model, which has the responsibility of deciding on MPRs. This fuzzy model assigns a fitness value to each flying node with regard to three metrics, namely remaining energy, neighboring degree, and link longevity. These metrics are directly proportional to the fitness value, meaning that if each of these metrics has a large value, the fitness value is also large, and hence, the corresponding flying node gets more chance to be MPR. 3) Topology discovery. This component defines the template of the enhanced topology control (TC) message, which has two additional fields (i.e. the energy and longevity of the relevant path). 4) Routing table. This component is tasked to decide on different paths in accordance with the energy and longevity inserted into the TC messages. The simulation results state that OLSR+ has successfully reduced delay, but it has a high routing overload. Additionally, OLSR+ has increased throughput and PDR compared to other schemes.

In [15], an energy-aware routing inspired by OLSR is suggested in FANETs. This algorithm tries to predict the quality of network connections according to two parameters, namely the ratio of received/sent hello packets and connection longevity. Moreover, this protocol employs the firefly algorithm (FA) for picking MPRs regarding four criteria, including connection quality, remaining energy, neighboring degree, and willingness. Each of these criteria has a direct relationship to the chance of MPR selection, meaning that if the criteria related to a flying node have large values, the chance of this node for selecting as MPR is high. Then, the routing protocol constructs the paths between different UAVs regarding the energy and connection quality of each path. The experiments performed in this paper show that this protocol works better than other schemes and improves consumed energy, latency, and throughput, but it increases the routing overhead in the network.

In [16], a link-optimized cone-assisted location (LoCaL) routing scheme is offered. This method attempts to increase the longevity of network links and choose relay nodes regarding remaining energy, link longevity, and safety degree. Paths formed in LoCaL are highly stable and consequently, these paths are less broken, and fewer interruptions occur in the data transfer operation between each source-destination pair. In addition, the authors propose a mathematical formula for the utility function, which enhances the route stability and picks relay nodes in a cone area. This lowers routing overhead when finding paths in the network. The simulation results indicate the superiority of LoCaL compared to other routing approaches.

In [17], a location-based routing approach called O-LAR is presented. This scheme improves location-aided routing (LAR). O-LAR defines a weight function to form the best route between flying nodes. Furthermore, this weight function decides on relay nodes with regard to remaining energy, distance, and movement direction. The performance of O-LAR is measured based on the simulation results. This scheme improves network longevity, throughput, link time, and PDR and decreases latency and routing overhead.

In [18], a location-based routing approach called LAR is offered to enhance the efficiency of routing strategies in mobile ad hoc networks. LAR regards the movement of nodes to adjust routing paths using an effective mechanism. According to this mechanism, LAR restricts the network environment based on the position of the destination to find routing paths in this limited area. Simulation results indicate that LAR can dramatically lower routing overhead because it applies the location information of nodes.

In [19], a greedy forwarding and limited flooding-based routing algorithm using the particle swarm optimization (PSO) called PSO-GLFR is designed for FANETs. This method is an improved sample of the greedy forwarding and flooding-based routing technique (GFR). PSO-GLFR defines two phases: PSO-based greedy forwarding and limited flooding. In the PSO-based greedy forwarding phase, the next-hop node is selected based on a cost function, which depends on three parameters, including distance to the destination, neighboring degree, and the difference between the movement angles of a flying node and the destination. In this cost function, the weights of the mentioned parameters are adjusted using the PSO algorithm. In the limited flooding strategy, an efficient flooding technique is designed to broadcast route requests and prevent routing holes. This strategy is limited based on a threshold value, which is dependent on maximum hops. The designed strategy can manage network congestion and energy consumed in the network. The experiments executed on PSO-GLFR indicate its efficiency, optimized energy consumption, and low latency in the network.

Most routing protocols provided in ad hoc networks such as FANET are only looking for the shortest route between the source and the destination, and ignore the features of these networks, especially the high mobility of UAVs and frequent link failures. Hence, they suffer often from high delay and overhead. Location-based routing methods such as LoCaL [16], O-LAR [17], and LAR [18] are more compatible with FANET because they utilize the geographic location information of UAVs. In addition, some routing protocols such as ICRA [12], TARRAQ [13], OLSR+ [14], Lansky et al. [15], LoCaL [16], and O-LAR [17] pay attention to the energy level when finding the next-hop node in the data transfer process because UAVs have limited energy capacity, which must be used for routing operations such as route discovery, route update, and route maintenance. If this energy capacity is not used correctly, UAVs lose their energy quickly. Therefore, FANETs need an energy-aware routing approach that considers the dynamic nature of drones and improves network performance.

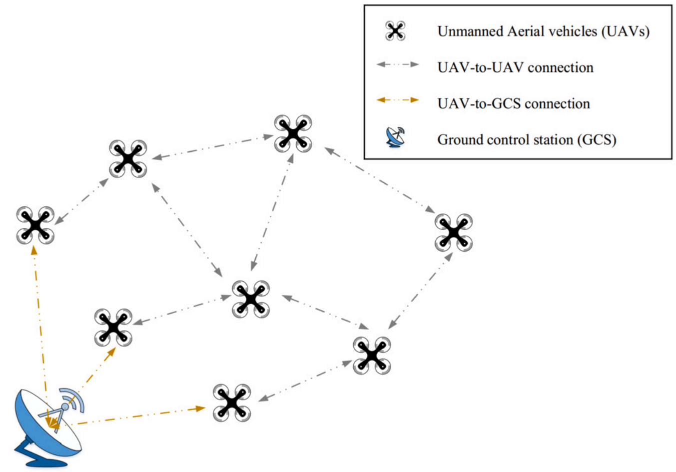


**Fig. 1.** Network model in EARVRT.

In this paper, an energy-aware routing based on a virtual relay tunnel (EARVRT) is presented in FANETs. In EARVRT, the route construction process is based on a virtual tunnel between source and destination. This virtual tunnel restricts the search space in the network and reduces routing overhead because only the drones inside the tunnel space are allowed to broadcast the route request (RREQ) message, other drones remove this message and do not participate in the routing process. This will greatly prevent the broadcast storm in the network. The construction of this tunnel is very fast and does not impose any extra overhead. EARVRT considers the energy status of each intermediate UAV in a routing path and introduces a new metric called the path correlation based on the two scales, including the cosine similarity of two nodes and their distance. Table 1 describes the most important features, strengths, and weaknesses of the routing methods presented in this section.

## 3. Network model

According to Fig. 1, the network model is a graph $G = (U, L)$ so that $U$ indicates a finite set of drones. This set is shown as $U = \{u_1, u_2, ..., u_N\}$. In addition, $L$ is a set of direct links available among drones. In the network, $u_i$ and $u_j$ are connected to each other either through a direct link (i.e. $u_i - to - u_j$) or through intermediate nodes (i.e. $u_i - \underbrace{u_p - \cdots - u_q}_{\text{Intermediate nodes}} - u_j$). Network assumptions are briefly stated below:

- A different ID (such as $Id_i$) is intended for each $u_i$ (where $i = 1, 2, ..., N$) to distinguish UAVs.
- All network links are bidirectional.
- UAVs support the communication standard IEEE.802.11g on the network.
- Each $u_i$ is equipped with a positioning system to determine its position at any given moment.
- Energy source and transmission radius of all UAVs are the same.
- The network includes a ground control station (GCS), which is connected directly to a number of UAVs at any moment.

## 4. Proposed scheme

Here, an energy-aware routing scheme based on a virtual relay tunnel (EARVRT) is offered for flying ad hoc networks. EARVRT is an

**Table 1**
Comparison of the related works.

| Scheme | Publication year | Energy-aware | Using position information | Routing criteria | Strengths | Weaknesses |
|---|---|---|---|---|---|---|
| LB-OPAR [11] | 2022 | × | ✓ | Path lifetime, path length, and network load | Not imposing any extra routing traffic to the network, finding the optimized path using a graph-based algorithm, presenting a lightweight algorithm, low communication overhead, and low computational complexity | Not considering energy efficiency in the routing process |
| ICRA [12] | 2022 | ✓ | ✓ | Using a greedy routing strategy based on the closest distance to destination | Considering energy efficiency, increasing the stability of network topology, low routing overhead, high scalability | Considering a fixed hello dissemination period, having fixed learning parameters such as learning rate and discount factor |
| TARRAQ [13] | 2022 | ✓ | ✓ | Based on link quality, energy, and distance between neighbors | Considering dynamic learning parameters, having low packet loss and low delay, considering energy in the routing operation, calculating link lifetime using Kalman filter | Low scalability, having a slow convergence speed, high time complexity, high computational complexity |
| OLSR+ [14] | 2022 | ✓ | ✓ | Presenting a fuzzy technique to calculate MPRs based on remaining energy, neighborhood degree, and link duration | Calculating a time-variant link duration, regarding energy efficiency in the routing operation, having a high network lifetime, creating the stability of paths | Not evaluating this scheme with regard to velocities of nodes, having high routing overhead |
| Lansky et al. [15] | 2023 | ✓ | ✓ | Using firefly algorithm in the MPR selection process based on remaining energy, neighborhood degree, and link duration | Regarding energy efficiency in the network, obtaining high network lifetime, calculating link quality regarding the number of hello packets and link duration, obtaining high stable routes in the network | Having high communication overhead, high time complexity, and slow convergence speed |
| LoCaL [16] | 2022 | ✓ | ✓ | Based on remaining energy, link duration time, and the closeness between two UAVs | Considering a three-dimensional cone-shaped architecture for reducing the forwarding area and lowering routing overhead, considering optimal energy consumption in the network | Not preventing routing holes |
| O-LAR [17] | 2021 | ✓ | ✓ | Based on remaining energy, distance, and movement angle | Improving the stability of paths, considering energy efficiency in network, restricting the network area in accordance with the position of the destination, managing routing overhead, adapting the LAR scheme to FANET | Limiting the RREQ distribution area using an ineffective and poor in FANET, high routing overhead |
| LAR [18] | 2000 | × | ✓ | Number of hops in the routing path | Restricting the network area in accordance with the position of the destination, managing routing overhead | Not suitable for FANET, not considering energy efficiency in the routing process, limiting the RREQ distribution area using an ineffective and poor in FANET, high routing overhead |
| PSO-GLFR [19] | 2019 | × | ✓ | Based on distance to the destination, neighboring degree, and the difference between movement angles | Presenting an efficient flooding technique, preventing routing holes due to the management of flooding of RREQs | High energy consumption due to the use of the PSO algorithm, high time complexity, not evaluation this scheme in different scenarios, high routing overhead |
| EARVRT | - | ✓ | ✓ | Path energy, the number of hops, and path correlation | Considering a virtual relay tunnel for reducing the forwarding area and decreasing routing overhead, considering energy efficiency in the network, calculating a new metric called path correlation | Need to improve network lifetime and energy consumption |

**Table 2**
Most important symbols used in this paper.

| Symbol | Description |
|---|---|
| $u_i$ | Flying node $i$ |
| $(x_i, y_i, z_i)$ | Spatial coordinates of $u_i$ |
| $Id_i$ | Identifier of $u_i$ |
| $u_s$ | Source UAV |
| $u_d$ | Destination UAV |
| $R$ | Transmission radius of UAVs in the network |
| RREQ | Route request message |
| RREP | Route reply message |
| $L$ | Line segment between $u_s$ and $u_d$ in a three dimensional network space |
| $Path_r$ | A path created between $u_s$ and $u_d$ |
| $PE_r$ | Energy of $Path_r$ |
| $CL_r$ | Correlation value of $Path_r$ |
| $d_{ij}$ | Distance between $u_i$ and $u_j$ |
| $cE_i$ | Total energy consumed by $u_i$ |
| $rE_i$ | Remaining energy of $u_i$ |
| $S_C(u_i, u_j)$ | Cosine similarity of these two UAVs in terms of the location status |
| $S_r$ | Score of $Path_r$ |

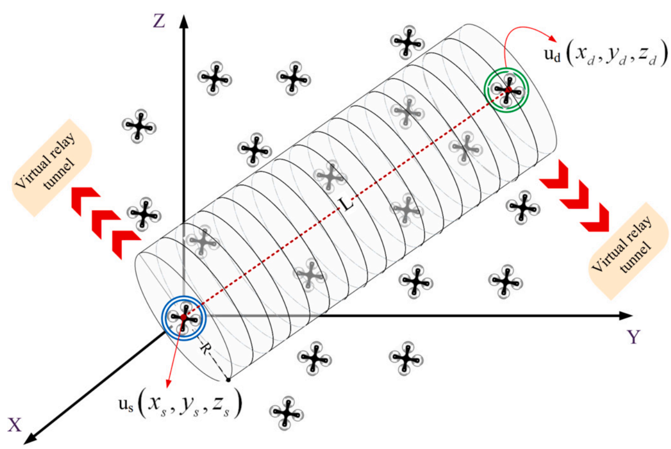


**Fig. 2.** The virtual tunnel between $u_s$ and $u_d$.

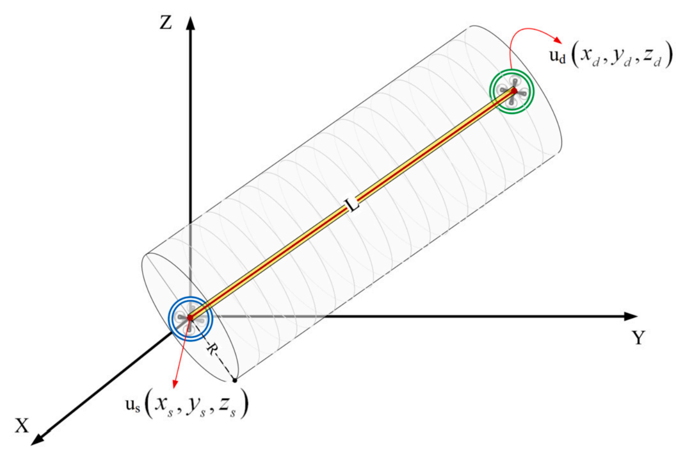


**Fig. 3.** Line segment between $u_s$ and $u_d$.

enhanced version of the AODV routing scheme and attempts to improve the adaptability of this method to the dynamic FANET environment and to deal with the problems caused by high routing overhead and the broadcast storm. In the suggested scheme, assume that the source UAV ($u_s$) decides to transfer data packets to the destination UAV ($u_d$). If $u_s$ cannot get a connected path in its routing table, it must build a new path between itself and $u_d$. To achieve this goal, $u_s$ constructs a virtual relay tunnel between itself and $u_d$. The purpose is to make a limited search space of the network and to decrease routing overhead. In general, EARVRT is formed of two steps:

- Creation of a virtual relay tunnel (VRT)
- VRT-based route discovery procedure

In the following, each of these two steps is described in detail. Table 2 defines the most important symbols used in this paper.

### 4.1. Virtual relay tunnel (VRT)

The VRT tunnel is a cylinder shape whose radius is $R$ (equivalent to the transmission radius of drones). This tunnel is drawn from $u_s$ to $u_d$. See Fig. 2. In EARVRT, only drones inside the tunnel space are allowed to broadcast the route request (RREQ) message and other drones must eliminate this message and not participate in the routing process. This idea lowers routing overhead. When designing this VRT tunnel, three points should be noted:

- The VRT tunnel must be efficient and effective in reducing routing overhead.
- The VRT construction procedure must not impose extra overhead because the main purpose of this tunnel is to reduce routing overhead.
- The VRT construction procedure must not require a long time interval.

The VRT tunnel is designed in two steps:

- **Step 1) Calculating the equation of the line segment (L):** In this step, several stages are done to obtain the formulation of the line segment $L$ located in the middle of the RVT tunnel between $u_s$ and $u_d$ with spatial coordinates $(x_s, y_s, z_s)$ and $(x_d, y_d, z_d)$, respectively. See Fig. 3
  - **1.** Get a vector such as $\overrightarrow{u_s u_d} = (x_d - x_s)\,i + (y_d - y_s)\,j + (z_d - z_s)\,k$, which is parallel to the line $L$.
  - **2.** Consider an arbitrary point $G(x, y, z)$ on the line segment $L$. Obviously, two vectors $\overrightarrow{u_s G}$ and $\overrightarrow{u_s u_d}$ are parallel to each other.
  - **3.** Now, as a general rule, it can be concluded that each point such as $G(x, y, z)$ is on the line $L$ if and only if $\overrightarrow{u_s G}$ is a multiplication of $\overrightarrow{u_s u_d}$:

$$\overrightarrow{u_s G} = \ell \overrightarrow{u_s u_d} \tag{1}$$

where $\ell$ is a numerical multiplier.
  - **4.** Equation (1) is rewritten according to its components to obtain Equation (2).

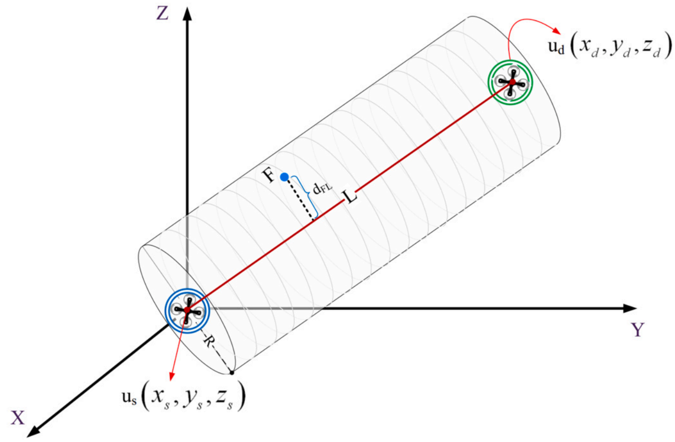


**Fig. 4.** Considering an arbitrary point like $F$ inside the VRT tunnel.

$$\left(x-x_s\right) i+\left(y-y_s\right) j+\left(z-z_s\right) k= \ell\left(x_d-x_s\right) i+\ell\left(y_d-y_s\right) j+\ell\left(z_d-z_s\right) k \tag{2}$$

Now, the corresponding components on both sides of Equation (2) are equal. As a result, Equations (3), (4), and (5) are obtained.

$$x-x_s=\ell\left(x_d-x_s\right) \rightarrow x=\ell\left(x_d-x_s\right)+x_s \tag{3}$$

$$y-y_s=\ell\left(y_d-y_s\right) \rightarrow y=\ell\left(y_d-y_s\right)+y_s \tag{4}$$

$$z-z_s=\ell\left(z_d-z_s\right) \rightarrow z=\ell\left(z_d-z_s\right)+z_s \tag{5}$$

- **5.** Based on Equations (3), (4), and (5), if $\ell=0$, the point $(x, y, z) = \left(\ell\left(x_d-x_s\right)+x_s, \ell\left(y_d-y_s\right)+y_s, \ell\left(z_d-z_s\right)+z_s\right)$ shows the position of $u_s$ $\left(x_s, y_s, z_s\right)$. Also, if $\ell=1$, $(x, y, z)=\left(\ell\left(x_d-x_s\right)+x_s, \ell\left(y_d-y_s\right)+y_s, \ell\left(z_d-z_s\right)+z_s\right)$ shows the position of $\left(x_d, y_d, z_d\right)$. Hence, we consider the condition $0 \leq \ell \leq 1$ to obtain the formula associated with the line segment $L$ based on Equation (6).

$$\begin{aligned} & x=\ell\left(x_d-x_s\right)+x_s, \\ & y=\ell\left(y_d-y_s\right)+y_s, \\ & z=\ell\left(z_d-z_s\right)+z_s, \qquad 0 \leq \ell \leq 1 \end{aligned} \tag{6}$$

- **Step 2) Determining the internal and external areas of the VRT tunnel:** In this step, consider an arbitrary point like $F\left(x_F, y_F, z_F\right)$ in the 3D network space. Now, the distance from $F$ to the line segment $L$ (i.e. $d_{FL}$) is calculated to determine whether $F$ is inside the VRT tunnel or not. View Fig. 4.
  - **1.** To get the distance $d_{FL}$, the first step is to find the spatial coordinates of the point $P$ on the line segment $L$, which has the least distance to $F$. The coordinates of $P$ i.e. $\left(x_P, y_P, z_P\right)$ is obtained according to Equation (7):

$$\left(x_P, y_P, z_P\right)=\left(\ell\left(x_d-x_s\right)+x_s, \ell\left(y_d-y_s\right)+y_s, \ell\left(z_d-z_s\right)+z_s\right) \tag{7}$$

  - **2.** To find the amount $\ell$, the squared distance between $P$ and $F$ is obtained according to Equation (8):

$$f(\ell)=\left(\ell\left(x_d-x_s\right)+x_s-x_F\right)^2+ \left(\ell\left(y_d-y_s\right)+y_s-y_F\right)^2+\left(\ell\left(z_d-z_s\right)+z_s-z_F\right)^2 \tag{8}$$

  - **3.** Obtain the derivative of $f(\ell)$ with respect to $\ell$ and place it equal to zero (i.e. $\frac{d f(\ell)}{d \ell}=0$). Then, the point $P$ is calculated according to the value $\ell$.
  - **4.** Calculate the distance between $F$ and $P$. Note that $d_{FL}$, which is also shown in Fig. 4, is the distance $F$ to the line segment $L$.
  - **5.** If $d_{FL} \leq R$, $F$ is inside the VRT tunnel.
  - **6.** If $d_{FL}>R$, $F$ is outside the VRT tunnel.

The VRT construction process is explained in Algorithm 1. Now, the time complexity of this algorithm is stated:

- Line 1 includes a command depending on Equation (6) whose time complexity is $O(1)$. Therefore, this command has a fixed execution time $c_1$.
- Line 2 is dependent on Equation (7), whose time complexity is $O(1)$. Hence, this command has a fixed execution time $c_2$.
- Line 3 is a command with a constant execution time $c_3$.
- Lines 4-8 include an *IF-THEN* condition and have a fixed runtime $c_4$.

According to the above, it can be found that the time complexity of Algorithm 1 is defined based on Equation (9):

$$T(n)=\sum_{i=1}^4 c_i \tag{9}$$

Therefore, the time complexity of this algorithm is $O(1)$.

**Algorithm 1** Virtual relay tunnel (VRT).

**Input:** $\left(x_s, y_s, z_s\right)$: Location of $u_s$
$\left(x_d, y_d, z_d\right)$: Location of $u_d$
$\left(x_F, y_F, z_F\right)$: Spatial coordinates of $F$
**Output:** RVT Tunnel
**Begin**
1: $\mathbf{u_s}$: Obtain the formulation of the line segment $L$ between $u_s$ and $u_d$ using Equation (6);
2: $\mathbf{u_s}$: Calculate the coordinates of the point $P$ on the line segment $L$ based on Equation (7);
3: $\mathbf{u_s}$: Compute the distance between the point $F$ and $P$;
4: **if** $d_{FL} \leq R$ **then**
5: $\mathbf{u_s}$: $F$ is inside the VRT Tunnel;
6: **else**
7: $\mathbf{u_s}$: $F$ is outside of the VRT tunnel;
8: **end if**
**End**

### 4.2. The VRT-based route discovery procedure

In EARVRT, when $u_s$ is looking for a connected path to transfer its data packets to $u_d$ and cannot obtain this path from its routing table, $u_s$ must search the network environment to form the appropriate path between itself and $u_d$. To achieve this goal, $u_s$ provides a RREQ message in accordance with the format presented in Fig. 5 and broadcasts it for the adjacent nodes such as $u_i$.

As shown in Fig. 5, all fields of RREQ in EARVRT, except four fields, including the energy of the relevant path ($PE_r$), the correlation of the relevant path ($CL_r$), coordinates of $u_s$ $\left(x_s, y_s, z_s\right)$, coordinates of $u_d$ $\left(x_d, y_d, z_d\right)$, are similar to those in AODV. In the following, these four fields are introduced.

- **Spatial coordinates of $\mathbf{u_s}$:** $u_s$ inserts its spatial coordinates in RREQ and this field does not change during the route discovery procedure.
- **Spatial coordinates of $\mathbf{u_d}$:** $u_s$ inserts the spatial coordinates of $u_d$ in RREQ and this field remains unchanged throughout the route discovery procedure.
- **The energy of the relevant path ($\mathbf{PE_r}$):** The energy status of each intermediate UAV, such as $u_i$ in the routing path, has a very important effect on network performance because if $u_i$ does not have enough energy, the whole path will be exposed to defeat. Hence, the routing process focuses on the energy needed for communications between UAVs. In FANET, communications between drones can be defined based on the free propagation model. Assume that $d_{ij}=\sqrt{\left(x_i-x_j\right)^2+\left(y_i-y_j\right)^2+\left(z_i-z_j\right)^2}$ is the distance between

| Message type | Hop count | $PE_r$ | $CL_r$ |
|---|---|---|---|
| Identifier of RREQ | | | |
| Spatial coordinates of $u_s$ $(x_s, y_s, z_s)$ | | | |
| Spatial coordinates of $u_d$ $(x_d, y_d, z_d)$ | | | |
| Destination IP address | | | |
| Sequence number of $u_d$ | | | |
| Source IP address | | | |
| Sequence number of $u_s$ | | | |

**Fig. 5.** Template of the RREQ message.

$u_i$ and $u_j$ with spatial coordinates $\left(x_i, y_i, z_i\right)$ and $\left(x_j, y_j, z_j\right)$, respectively. $l$ bits are sent from $u_i$ to $u_j$. The consumed energy of $u_i$ (the transmitter) is estimated based on Equation (10).

$$E_i^{sent}\left(l, d_{ij}\right) = l \times E_{elec} + l \times \varepsilon_{fs} \times d_{ij}^2 \tag{10}$$

Also, the energy consumed of $u_j$ (receiver) is obtained through Equation (11).

$$E_j^{received}(l) = l \times E_{elec} \tag{11}$$

where $E_{elec}$ is the energy consumed by the recipient/transmitter circuit to receive/send each bit. $\varepsilon_{fs}$ indicates the coefficient of amplifier in the free space.

According to the mentioned content above, the total energy consumed by $u_i$ ($cE_i$) is measured in accordance with the energy used in the data transfer operations (transmission/reception) performed by $u_i$ until the present moment.

$$cE_i = \sum_{k=1}^{n_T}\left(E_i^{sent,k} + E_i^{received,k}\right) \tag{12}$$

where $n_T$ indicates the number of data transfer operations performed by $u_i$ until the present moment. Furthermore, the remaining energy of $u_i$ ($rE_i$) is equal to:

$$rE_i = E_{\max} - cE_i \tag{13}$$

Here, $E_{\max}$ is the initial energy of drones.

The energy of the route ($PE_r$) is affected by the residual energy of the UAVs available in that path, so an intermediate node with the lowest residual energy compared to other intermediate nodes is known as the crisis point of the path, which affects the longevity of the path. Hence, the energy of $Path_r$ (i.e. $PE_r$) is equal to the residual energy of the crisis point:

$$PE_r = \min_{u_i \in Path_r}\left\{rE_i\right\} \tag{14}$$

- **The correlation of the relevant path ($\mathbf{CL_r}$):** The spatial correlation of two consecutive nodes $u_i$ and $u_j$ in the routing path is a significant parameter, which has a great effect on network performance because if $u_i$ and $u_j$ are out of each other's communication range, this results in the cut off of the routing path. Spatial correlation of $u_i$ and $u_j$ is obtained from the location information of these two nodes through Equation (15).

$$CL\left(u_i, u_j\right) = \begin{cases} \frac{1}{2}\left(\left|S_C\left(u_i, u_j\right)\right| + 1\right)\left(\frac{R + d_{ij}^t}{R}\right), & d_{ij}^t - d_{ij}^{t-1} \le 0 \\ \frac{1}{2}\left(S_C\left(u_i, u_j\right) + 1\right)\left(\frac{R - d_{ij}^t}{R}\right), & d_{ij}^t - d_{ij}^{t-1} > 0 \end{cases} \tag{15}$$

where $R$ is the transmission radius of $u_i$ and $u_j$. Also, $S_C\left(u_i, u_j\right)$ is the cosine similarity of these two UAVs in terms of the location status. It is calculated through Equation (16).

$$S_C\left(u_i, u_j\right) = \frac{x_i x_j + y_i y_j + z_i z_j}{\sqrt{{x_i}^2 + {y_i}^2 + {z_i}^2} \times \sqrt{{x_j}^2 + {y_j}^2 + {z_j}^2}} \tag{16}$$

So, $\left(x_i, y_i, z_i\right)$ and $\left(x_j, y_j, z_j\right)$ show the coordinates of $u_i$ and $u_j$, respectively. Note that $S_C\left(u_i, u_j\right) \in [-1, 1]$ meaning that if the movement vectors of $u_i$ and $u_j$ are similar to each other and the angle between the two vectors is close to zero, $S_C\left(u_i, u_j\right)$ is close to one. Whereas, if the two vectors are dissimilar and the angle between the two vectors is close to $\pi$, in this case, $S_C\left(u_i, u_j\right)$ is closer to $-1$.

In Equation (15), the phrase $\frac{1}{2}\left(S_C\left(u_i, u_j\right) + 1\right)$ is intended to limit $S_C\left(u_i, u_j\right)$ in $[0, 1]$. Also, $d_{ij}^t = \sqrt{\left(x_i - x_j\right)^2 + \left(y_i - y_j\right)^2 + \left(z_i - z_j\right)^2}$ reflects the distance between $u_i$ and $u_j$ at moment $t$. If $u_i$ and $u_j$ are approaching each other and $d_{ij}^t - d_{ij}^{t-1} \le 0$, the correlation between $u_i$ and $u_j$ is increasing (the first relationship in Equation (15)). Otherwise, the correlation between $u_i$ and $u_j$ is lowering (the second relationship in Equation (15)).

As a result, the correlation of $Path_r$ ($CL_r$) is equal to the lowest correlation between two consecutive UAVs in that path. Note that if the correlation of a path is higher, this path is more stable.

$$CL_r = \min_{u_i, u_j \in Path_r}\left\{CL\left(u_i, u_j\right)\right\} \tag{17}$$

When $u_i$ receives the RREQ, it examines its status in accordance with Section 4.1 and repeats the RREQ distribution process if it is inside the VRT tunnel. Otherwise, $u_i$ will remove the RREQ. See Fig. 6. According to this figure, $u_s$ disseminate RREQ to five nodes, namely $u_1$, $u_2$, $u_3$, $u_4$, and $u_5$. Only two nodes $u_2$ and $u_3$ are inside the VRT tunnel and can broadcast the RREQ message but $u_1$, $u_4$, and $u_5$ are outside of the VRT tunnel and must discard RREQ.

The RREQ broadcast process is finished when it arrives $u_d$. See Fig. 7. Then, $u_d$ employs Equation (18) to get the score $S_r$ for each created route such as $ROUTE_1 : u_s - u_2 - u_8 - u_{14} - u_d$ and $ROUTE_2 : u_s - u_3 - u_9 - u_{15} - u_d$ in Fig. 8 and returns a route reply (RREP) message to $u_s$ through the path with the highest $S_r$ (i.e. $ROUTE_1$). See Fig. 9. Finally, $u_s$ holds this path in its routing table and applies the route maintenance technique similar to that in AODV to identify and modify the broken paths in its routing table.

$$S_r = \omega_1 PE_r + \omega_2 CL_r + \omega_3\left(1 - H_r\right) \tag{18}$$

where $PE_r$, $CL_r$, and $H_r$ indicate the energy, correlation, and the number of hops related to $Path_r$, respectively. Also, $\omega_1$, $\omega_2$, and $\omega_3$ represent weight coefficients and $\sum_{i=1}^{3}\omega_i = 1$.

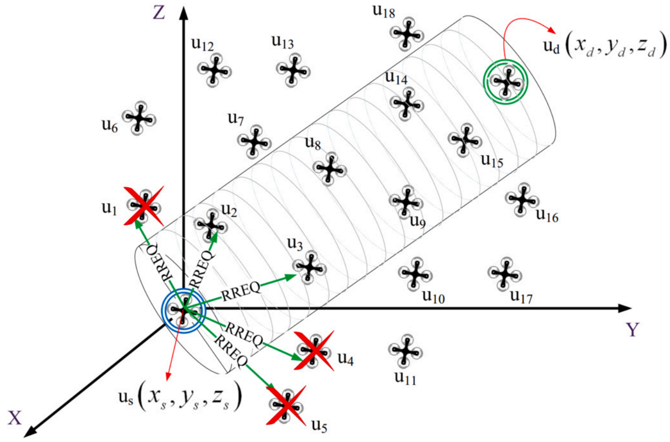


**Fig. 6.** Route discovery process and filtering the nodes, which are out of the VRT tunnel.

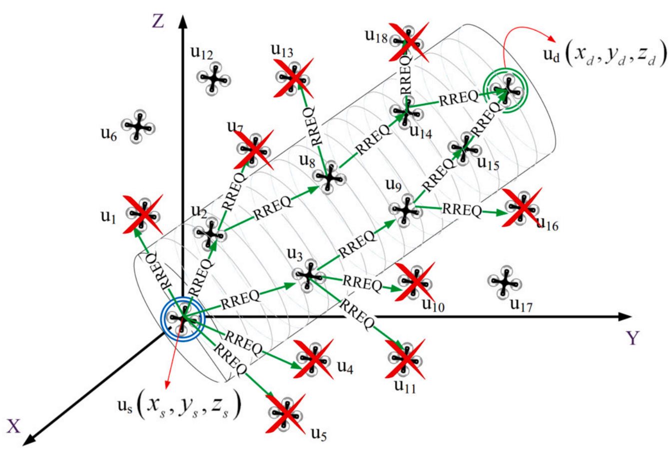


**Fig. 7.** Route discovery process and finding routes to $u_d$.

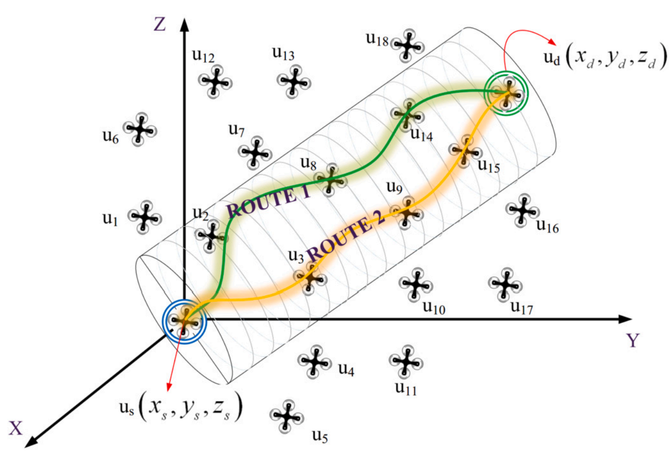


**Fig. 8.** Created paths in the route discovery process.

Algorithm 2 describes the VRT-based route discovery process. In the following, we explain the time complexity of this algorithm:

- In Line 1, a command with a fixed run time $q_1$ is presented.
- Line 2 defines a *REPEAT-UNTIL* loop to repeat the route discovery process in the simulation time.
- In Line 3, an *IF-THEN* condition states the execution condition of the route discovery process. This condition includes the following commands:

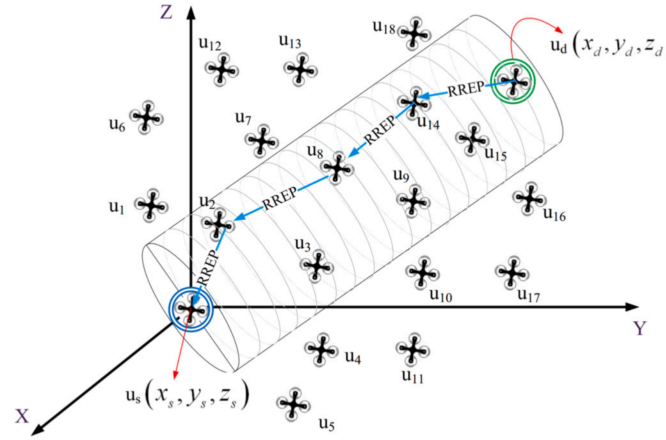


**Fig. 9.** Sending RREP message to $u_s$ via $ROUTE_1$.

– Line 4 contains a command to produce RREQ. It has a fixed runtime $q_2$.
– Line 5 contains a command to disseminate RREQ. It has a constant runtime $q_3$.
– Line 6 includes a *WHILE* loop to repeat the RREQ dissemination process. This loop is repeated $N-1$ times so that $N$ is equal to the number of nodes. It includes the following commands.
  * Line 7 depends on Equations (14) and (17) and has a constant implementation time $q_4$.
  * Line 8 has a command with a fixed run time $q_5$.
  * Line 9 depends on Algorithm 1 whose time complexity is $O(1)$. As a result, it has a constant execution time $q_6$.
  * Lines 10-13 include an *IF-THEN* condition, which is executed in a fixed run time $q_7$.

  Therefore, the time complexity of the *WHILE* loop is defined based on Equation (19):

$$T_{While}(n) = (N-1)\left(\sum_{i=4}^{7} q_i\right) \tag{19}$$

  Suppose there is a positive number like $q$ and $q > \left(\sum_{i=4}^{7} q_i\right)$.

  Therefore:

$$T_{While}(n) = (N-1)\left(\sum_{i=4}^{7} q_i\right) < (N-1)\,q \tag{20}$$

– In lines 15-18, there are an *IF-THEN* command, which consists of two commands, the first command depends on Equation (18) and has a fixed execution time $q_8$, and the second command has a fixed execution time $q_9$.

So the time complexity of *IF-THEN* command is equal to:

$$T_{IF}(n) = q_2 + q_3 + (N-1)\,q + q_8 + q_9 \tag{21}$$

Suppose there is a positive number like $f$ and $f > q_2 + q_3 + q + q_8 + q_9$:

$$T_{IF}(n) = q_2 + q_3 + (N-1)\,q + q_8 + q_9 < (N-1)\,f \tag{22}$$

As a result, the total time complexity of Algorithm 2 is $O(N)$, and $N$ indicates the total number of nodes in the network.

## 5. Simulation and results evaluation

Here, the evaluation of the results related to EARVRT obtained from its simulation in NS2 is presented. In this process, several UAVs (between 5-30) are regarded in the network environment whose dimensions are $1 \times 1 \times 1\ \text{km}^3$. The speed change interval, the transfer radius,

**Algorithm 2** VRT-based route discovery process.

**Input:** $u_s$: Source UAV
$u_d$: Destination UAV
$u_i$: Intermediate node
$T_{net}$: Time spent in the network
$T_{Sim}$: Simulation time
**Output:** A suitable path between $u_s$ and $u_d$.
**Begin**
Set $T_{net} = 0$;
**repeat**
  **if** $u_s$ cannot find a valid path to $u_d$ in its routing table **and** $u_s$ has a packet for $u_d$ **then**
    $\mathbf{u_s}$: Produce a route request (RREQ) packet according to the format presented in Fig. 5;
    $\mathbf{u_s}$: Disseminate RREQ for intermediate nodes such as $u_i$;
    **while** $u_d$ receives RREQ **do**
      $\mathbf{u_i}$: Update the fields of $PE_r$ and $CL_r$ in RREQ based on Equations (14) and (17), respectively;
      $\mathbf{u_i}$: Add one unit to $H_r$;
      $\mathbf{u_i}$: **call** Algorithm 1;
      **if** $u_i$ is inside the VRT tunnel **then**
        $\mathbf{u_i}$: Replace the next-hop node with $u_i$;
        $\mathbf{u_i}$: Disseminate RREQ for its neighboring nodes;
      **end if**
    **end while**
    **if** $u_d$ receives RREQ **then**
      $\mathbf{u_d}$: Calculate $S_r$ for each $Path_r$ created between $u_s$ and $u_d$ based on Equation (18);
      $\mathbf{u_d}$: Send Back a route reply packet to $u_s$ through $Path_r$ with the highest $S_r$;
    **end if**
  **end if**
  $T_{net} = T_{net} + 1$;
**until** $T_{net} \leq T_{Sim}$
**End**

and the initial energy of the UAVs are 10 – 110 m/s, 250 meters, and 100 joules, respectively. Note that simulation operations include two experimental scenarios, namely change in network density and change in the flight speed of UAVs.

- In the first scenario, namely change in the network density, it is assumed that the speed of UAVs is fixed at 60 m/s to evaluate the effect of change in the number of nodes in the network performance in terms of the five criteria, namely energy consumption, packet delivery rate, network lifetime, routing overhead, and delay.
- In the second scenario, namely change in the speed of UAVs, it is assumed that the number of nodes is fixed on 10 to evaluate the effect of change in the speed of flying nodes on network performance in terms of the five criteria mentioned above.

To enhance the accuracy of the results, the experiments have been done 10 times and the average value is presented as the result. In these experiments, the results related to five criteria, namely energy consumption, packet delivery rate, network longevity, overhead, and delay in three methods, namely LoCaL [16], O-LAR [17], and PSO-GLFR [19] are compared with those in EARVRT. Review the simulation scales in Table 3.

### 5.1. Energy consumption (EC)

Fig. 10 shows the energy consumed in various schemes when changing the number of flying nodes. In this experiment, it is assumed that the speed of the UAVs is adjusted on a fixed value (i.e. 60 m/s). According to this figure, EARVRT has the best energy consumption, which is 10.40%, 23.43%, and 24.80% lower than LoCaL, O-LAR, and PSO-GLFR, respectively. On the other hand, Fig. 11 has tested the energy consumed in these schemes regarding different flight speeds. In this figure, the number of network nodes is 10. According to this figure, energy consumption in EARVRT and LoCaL is very close to each other so

**Table 3**
Simulation settings.

| Scale | Value |
|---|---|
| Simulator | NS2 |
| Compared schemes | LoCaL, O-LAR, PSO-GLFR |
| Network dimensions | $1 \times 1 \times 1\,\text{km}^3$ |
| The number of flying nodes | 5-30 |
| Mobility model | Random waypoint |
| Transmission radius | 250 meters |
| Flight speed | 10 – 110 m/s |
| Initial energy | 100 Joule |
| Runtime | 150 seconds |
| MAC layer protocol | IEEE 802.11 g |
| Transmission power | 10 dBm |
| Packet size | 512 bytes |
| Traffic model | Constant bit rate (CBR) |
| Traffic rate | 2 Mbps |

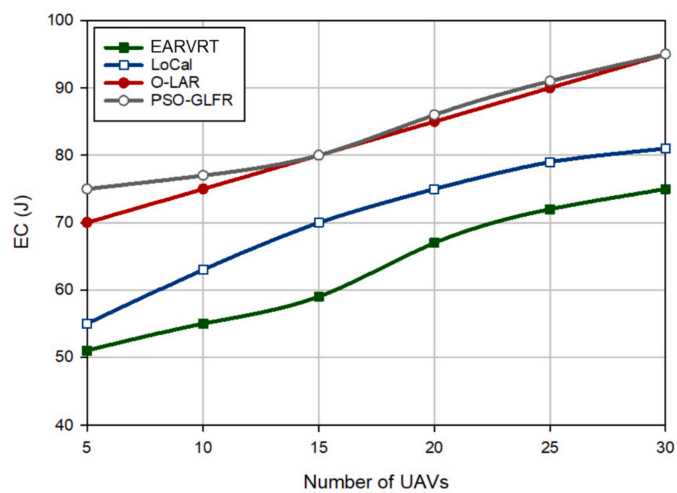


**Fig. 10.** Energy consumption according to the number of flying nodes.

our scheme has lowered energy consumption by 1.52%, 11.91%, and 13.43% compared to LoCaL, O-LAR, and PSO-GLFR, respectively. This is because EARVRT restricts the RREQ broadcast area using the virtual tunnel and considers energy consumption in the route selection operation. LoCaL is energy-efficient because it utilizes a restriction technique to limit the RREQ broadcast area. While O-LAR has limited the RREQ distribution area, its restriction technique is ineffective and poor in FANET. PSO-GLFR is energy-consuming due to the use of the PSO algorithm, and on the other hand, the flooding of RREQ is limited solely to the number of hops. This restriction technique can prevent routing holes, but the flying nodes experience high energy usage.

### 5.2. Network routing overhead (NRO)

In Fig. 12, the overhead is tested in different approaches by taking into account a fixed flight speed (i.e. 60 m/s) and changing the density of flying nodes. According to this figure, the routing overhead of EARVRT is 15.38%, 33.33%, and 39.89% lower than LoCaL, O-LAR, and PSO-GLFR, respectively. Fig. 13 also shows the overhead in different schemes by adjusting the number of UAVs on 10 and changing the flight speed of UAVs. As shown in this figure, EARVRT has reduced the routing overhead by 20%, 40.48%, and 44.44% compared to LoCaL, O-LAR, and PSO-GLFR, respectively. The virtual tunnel designed in EARVRT and the management of the relay UAVs reduce the overhead. Additionally, the route selection mechanism in our method is looking for high-energy and correlated paths. Hence, the constructed paths will have good stability, which lowers the number of broken routes. This reduces the need for new paths, which lowers the routing overhead in the path discovery process.

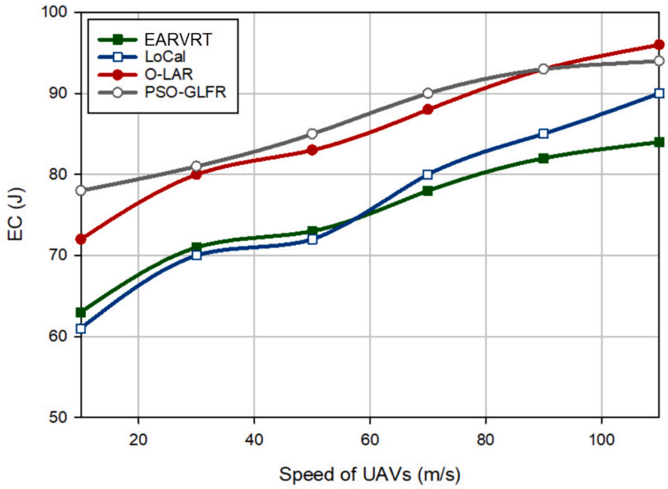


**Fig. 11.** Energy consumption with respect to the flight speed of nodes.

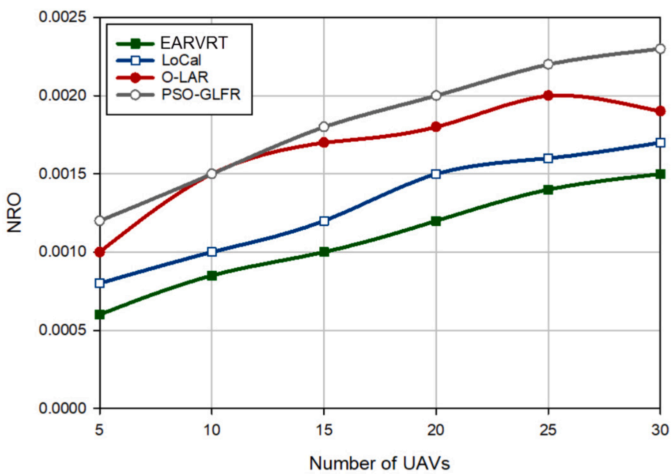


**Fig. 12.** Routing overhead regarding the number of flying nodes.

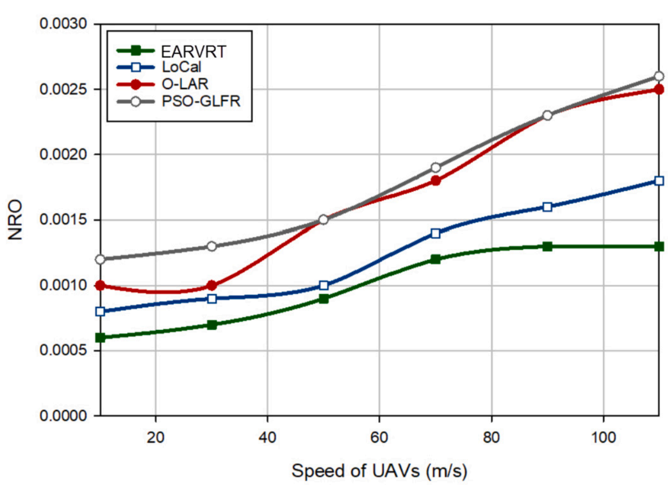


**Fig. 13.** Routing overhead regarding different flight speeds.

### 5.3. Message delivery rate (MDR)

In Fig. 14, the packet delivery rate is shown in various approaches by considering a constant flight speed equal to 60 m/s and varying the density of UAVs. The experiment proves that EARVRT has improved MDR by 3.11%, 11.076%, and 12.62% in comparison with LoCaL, O-LAR, and PSO-GLFR, respectively. In Fig. 14, MDR is directly proportional to the node density, meaning that if the density of the nodes is high, MDR will be also high and vice versa. The reason is that the high density of UAVs increases the chance of finding appropriate and stable paths between the nodes. As a result, there are fewer broken paths, which lower missing packets caused by the disconnected links. Furthermore, Fig. 15 analyzes the results of MDR in various routing approaches by taking into account 10 nodes and changing the speed of UAVs. According to this figure, EARVRT has increased this scale by 6.38%, 14.80%, and 18.65% compared with LoCaL, O-LAR, and PSO-GLFR, respectively. In Fig. 15, MDR and flight speed have an opposite relationship, meaning that the faster UAVs experience less MDR because higher speed will increase the number of broken links between UAVs, and consequently, more packets are lost.

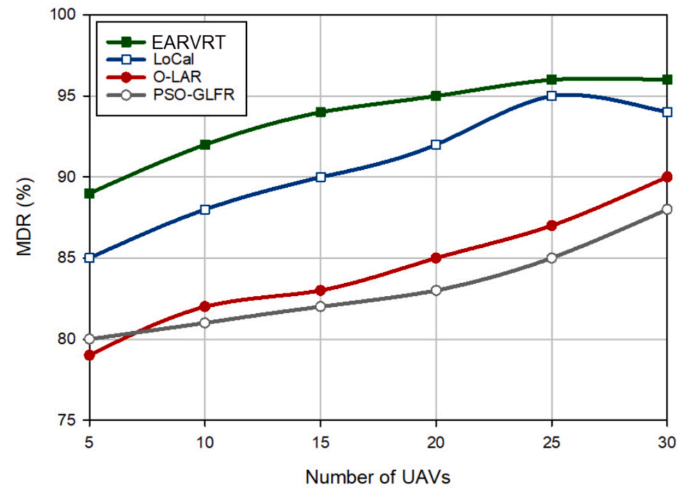


**Fig. 14.** Message delivery rate based on the number of UAVs.

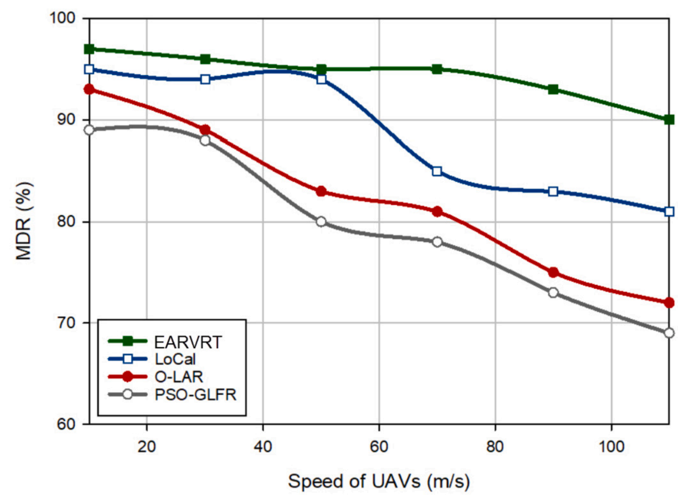


**Fig. 15.** Message delivery rate with respect to the change in flight speed.

### 5.4. Network Longevity (NL)

In Fig. 16, the results of network longevity are stated in different schemes, when considering a fixed speed equal to 60 m/s and changing the density of UAVs. The experiment shows that network longevity in EARVRT is about 3.36% less than that in LoCaL. However, our scheme has improved this scale by 3.84% and 14.16% compared to O-LAR and PSO-GLFR, respectively. According to Fig. 17, this is also true for evaluating network longevity for 10 nodes with different flight speeds so that this scale in EARVRT is approximately 0.97% less than LoCaL, and

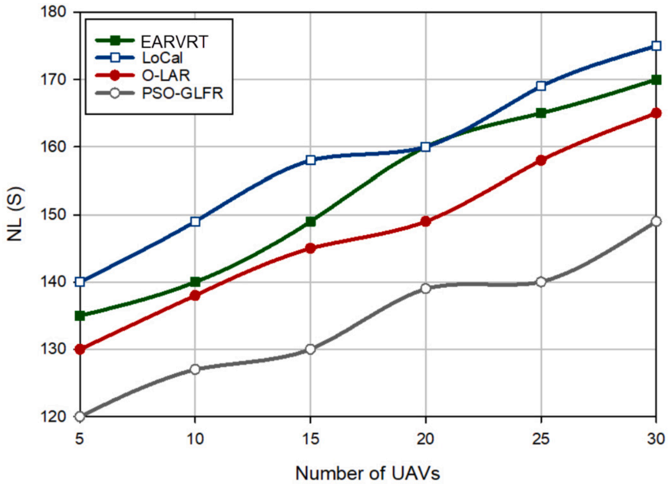


**Fig. 16.** Network longevity in accordance with the number of flying nodes.

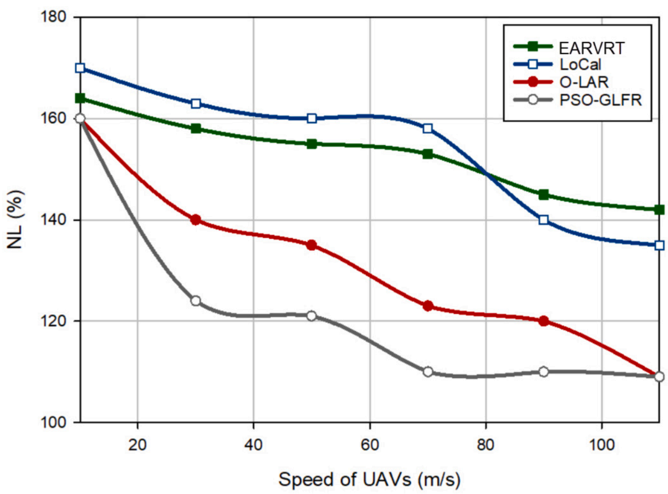


**Fig. 17.** Network longevity with regard to the flight speed of UAVs.

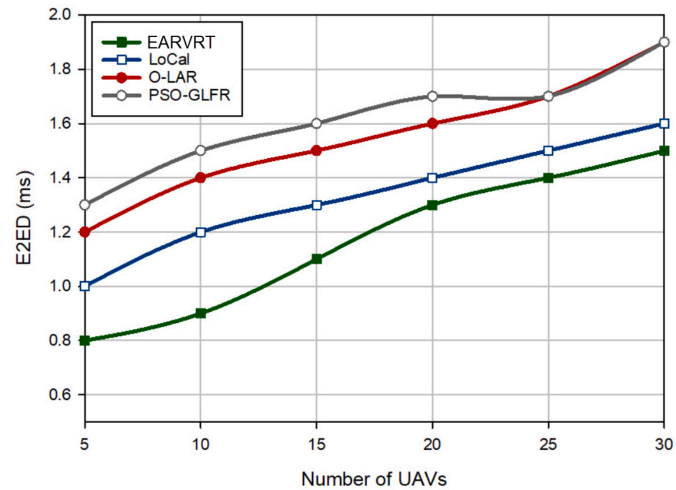


**Fig. 18.** Delay according to the number of network nodes.

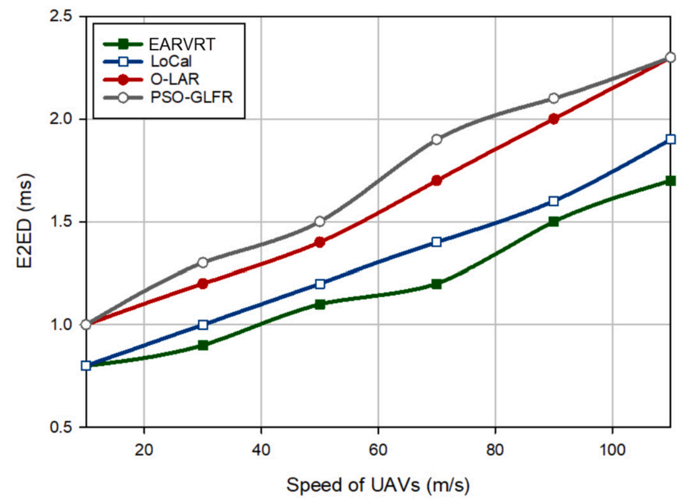


**Fig. 19.** Delay with regard to the flight speed of UAVs.

EARVRT increases network longevity by 16.51% and 24.93% compared to O-LAR and PSO-GLFR, respectively. The reasons for this issue were accurately stated in Section 5.1 when evaluating energy consumption on the network.

### 5.5. End-to-end delay (E2ED)

Fig. 18 evaluates delay in different schemes when changing the number of nodes and adjusting the flight speed to 60 m/s. This figure shows that delay in EARVRT is 12.03%, 24.52%, and 27.78% less than LoCaL, O-LAR, and PSO-GLFR because our scheme considers the spatial correlation of UAVs available in the path to choose more stable paths for data transfer. As a result, data packets arrive at the destination in the fastest possible time. On the other hand, the virtual tunnel lowers routing overhead. This will help reduce delay in the proposed scheme. In Fig. 19, delay in various schemes is tested for 10 nodes and different flight speeds. According to this figure, EARVRT will reduce delay by 9.09%, 25%, and 28.57% compared to LoCaL, O-LAR, and PSO-GLFR, respectively. Based on Fig. 19, the faster UAVs experience a higher delay in different schemes. This leads to a high number of broken paths, which need to discover new routes between UAVs.

## 6. Conclusion

In this paper, an energy-aware routing scheme based on a virtual relay tunnel (EARVRT) is proposed in flying ad hoc networks. This method is formed of two steps: virtual relay tunnel (VRT) and route selection. When building a VRT tunnel, the relay nodes are filtered in the route discovery process to manage routing overhead. On the other hand, the routing path is picked according to the energy of the path, hop counts, and the correlation of the path. EARVRT is simulated in NS2 and its performance is measured in two experimental scenarios, namely the change of network density and the variation of the flight speed. In the first scenario including the change of network density, EARVRT has improved the consumed energy by 10.40%, 23.43%, and 24.80%, routing overhead by 15.38%, 33.33%, and 39.89%, PDR by 31.3%, 11.076%, and 12.62%, and delay by 12.03%, 24.52%, and 27.78% in comparison with LoCaL, O-LAR, and PSO-GLFR, respectively. However, network longevity in EARVRT is about 3.36% less than that in LoCaL. In the second experimental scenario including the change in flight speed, our scheme has improved energy consumption by 1.52%, 11.91%, and 13.43%, routing overhead by 20%, 40.48%, and 44.44%, PDR by 6.38%, 14.80%, and 18.65%, and delay by 9.09%, 25%, and 28.57% compared to LoCaL, O-LAR, and PSO-GLFR, respectively. However, EARVRT has about 0.97% lower network lifetime than LoCaL. In future research directions, the routing process is improved using machine learning (ML) methods and optimization algorithms to reduce routing overhead more. Also, ML techniques such as Q-learning can be used for building an intelligent virtual relay tunnel to reduce routing overhead and make more stable paths. This intelligent tunnel is not merely cylindrical and varies in its radius or direction according to the network conditions.

## Declaration of competing interest

We declare no financial, personal, professional, or other conflicts of interest that could influence the work reported in this manuscript.


## Acknowledgements

The result was created through solving the student project “Security analysis and developing lightweight ciphers and protocols” using objective-oriented support for specific university research from the University of Finance and Administration, Prague, Czech Republic. Authors thank Michal Merta, and Zdenek Truhlar for their help with the research connected with the topic of the article.


## References


[1] F. Pasandideh, J.P.J.D. Costa, R. Kunst, W. Hardjawana, E.P. de Freitas, A systematic literature review of flying ad hoc networks: state-of-the-art, challenges, and perspectives, J. Field Robot. (2023), https://doi.org/10.1002/rob.22157.

[2] J. Lansky, S. Ali, A.M. Rahmani, M.S. Yousefpoor, E. Yousefpoor, F. Khan, M. Hosseinzadeh, Reinforcement learning-based routing protocols in flying ad hoc networks (FANET): a review, Mathematics 10 (16) (2022) 3017, https://doi.org/10.3390/math10163017.

[3] A. Rovira-Sugranes, A. Razi, F. Afghah, J. Chakareski, A review of AI-enabled routing protocols for UAV networks: trends, challenges, and future outlook, Ad Hoc Netw. 130 (2022) 102790, https://doi.org/10.1016/j.adhoc.2022.102790.

[4] J. Agrawal, M. Kapoor, A comparative study on geographic-based routing algorithms for flying ad-hoc networks, Concurr. Comput., Pract. Exp. 33 (16) (2021) e6253, https://doi.org/10.1002/cpe.6253.

[5] S.W. Lee, S. Ali, M.S. Yousefpoor, E. Yousefpoor, P. Lalbakhsh, D. Javaheri, A.M. Rahmani, M. Hosseinzadeh, An energy-aware and predictive fuzzy logic-based routing scheme in flying ad hoc networks (fanets), IEEE Access 9 (2021) 129977–130005, https://doi.org/10.1109/ACCESS.2021.3111444.

[6] S. Gangopadhyay, V.K. Jain, A position-based modified OLSR routing protocol for flying ad hoc networks, IEEE Trans. Veh. Technol. (2023), https://doi.org/10.1109/TVT.2023.3265704.

[7] Y. Cheriguene, F.Z. Bousbaa, C.A. Kerrache, S. Djellikh, N. Lagraa, M. Lahby, A. Lakas, COCOMA: a resource-optimized cooperative UAVs communication protocol for surveillance and monitoring applications, Wirel. Netw. (2022) 1–17, https://doi.org/10.1007/s11276-022-03031-8.

[8] Z. Ma, Q. Guo, J. Ma, Z. Zhang, H. Ma, L. Peng, Y. Li, VaSe-MRP: velocity-aware and stability-estimation–based multi-path routing protocol in flying ad hoc network, Int. J. Distrib. Sens. Netw. 15 (11) (2019) 1550147719883128, https://doi.org/10.1177/1550147719883128.

[9] F. Syed, S.K. Gupta, S. Hamood Alsamhi, M. Rashid, X. Liu, A survey on recent optimal techniques for securing unmanned aerial vehicles applications, Trans. Emerg. Telecommun. Technol. 32 (7) (2021) e4133, https://doi.org/10.1002/ett.4133.

[10] B. Zheng, K. Zhuo, H. Zhang, H.X. Wu, A novel airborne greedy geographic routing protocol for flying ad hoc networks, Wirel. Netw. (2022) 1–15, https://doi.org/10.1007/s11276-022-03030-9.

[11] M. Gharib, F. Afghah, E.S. Bentley, LB-OPAR: load balanced optimized predictive and adaptive routing for cooperative UAV networks, Ad Hoc Netw. 132 (2022) 102878, https://doi.org/10.1016/j.adhoc.2022.102878.

[12] J. Guo, H. Gao, Z. Liu, F. Huang, J. Zhang, X. Li, J. Ma, ICRA: an intelligent clustering routing approach for UAV ad hoc networks, IEEE Trans. Intell. Transp. Syst. (2022), https://doi.org/10.1109/TITS.2022.3145857.

[13] Y. Cui, Q. Zhang, Z. Feng, Z. Wei, C. Shi, H. Yang, Topology-aware resilient routing protocol for FANETs: an adaptive Q-learning approach, IEEE Int. Things J. 9 (19) (2022) 18632–18649, https://doi.org/10.1109/JIOT.2022.3162849.

[14] A.M. Rahmani, S. Ali, E. Yousefpoor, M.S. Yousefpoor, D. Javaheri, P. Lalbakhsh, O.H. Ahmed, M. Hosseinzadeh, S.W. Lee, OLSR+: a new routing method based on fuzzy logic in flying ad-hoc networks (FANETs), Veh. Commun. 36 (2022) 100489, https://doi.org/10.1016/j.vehcom.2022.100489.

[15] J. Lansky, A.M. Rahmani, M.H. Malik, E. Yousefpoor, M.S. Yousefpoor, M.U. Khan, M. Hosseinzadeh, An energy-aware routing method using firefly algorithm for flying ad hoc networks, Sci. Rep. 13 (1) (2023) 1323, https://doi.org/10.1038/s41598-023-27567-7.

[16] S. Kumar, R.S. Raw, A. Bansal, LoCaL: link-optimized cone-assisted location routing in flying ad hoc networks, Int. J. Commun. Syst. 36 (2) (2023) e5375, https://doi.org/10.1002/dac.5375.

[17] S. Kumar, R.S. Raw, A. Bansal, M.A. Mohammed, P. Khuwuthyakorn, O. Thinnukool, 3D location oriented routing in flying ad-hoc networks for information dissemination, IEEE Access 9 (2021) 137083–137098, https://doi.org/10.1109/ACCESS.2021.3115000.

[18] Y. Ko, N.H. Vaidya, Location-Aided Routing (LAR) in mobile ad hoc networks, Wirel. Netw. 6 (2000) 307–321, https://doi.org/10.1023/A:1019106118419.

[19] F. Wang, Z. Chen, J. Zhang, C. Zhou, W. Yue, Greedy forwarding and limited flooding based routing protocol for UAV flying ad-hoc networks, in: 2019 IEEE 9th International Conference on Electronics Information and Emergency Communication (ICEIEC), IEEE, July 2019, pp. 1–4.

[20] C. Perkins, E. Belding-Royer, S. Das, RFC3561: ad hoc on-demand distance vector (AODV) routing, https://doi.org/10.17487/RFC3561, 2003.

[21] M. Hosseinzadeh, J. Tanveer, L. Ionescu-Feleaga, B.S. Ionescu, M.S. Yousefpoor, E. Yousefpoor, O.H. Ahmed, A.M. Rahmani, A. Mehmood, A greedy perimeter stateless routing method based on a position prediction mechanism for flying ad hoc networks, J. King Saud Univ, Comput. Inf. Sci. (2023) 101712, https://doi.org/10.1016/j.jksuci.2023.101712.

[22] J. Lansky, A.M. Rahmani, M. Hosseinzadeh, Reinforcement learning-based routing protocols in vehicular ad hoc networks for intelligent transport system (ITS): a survey, Mathematics 10 (24) (2022) 4673, https://doi.org/10.3390/math10244673.

[23] A.M. Rahmani, R.A. Naqvi, E. Yousefpoor, M.S. Yousefpoor, O.H. Ahmed, M. Hosseinzadeh, K. Siddique, A Q-learning and fuzzy logic-based hierarchical routing scheme in the intelligent transportation system for smart cities, Mathematics 10 (22) (2022) 4192, https://doi.org/10.3390/math10224192.

[24] M.U. Khan, M. Hosseinzadeh, A. Mosavi, An intersection-based routing scheme using Q-learning in vehicular ad hoc networks for traffic management in the intelligent transportation system, Mathematics 10 (20) (2022) 3731, https://doi.org/10.3390/math10203731.